TECHNICAL REPORT ARLCB-TR-82020

FRACTURE MECHANICS ANALYSIS OF THE EFFECTS OF RESIDUAL STRESS ON FATIGUE LIFE

Joseph F. Throop

July 1982

US ARMY ARMAMENT RESEARCH AND DEVELOPMENT COMMAND
LARGE CALIBER WEAPON SYSTEMS LABORATORY
BENÉT WEAPONS LABORATORY
WATERVLIET, N. Y. 12189

AMCMS No. 611102H600011

DA Project No. 1L161102AH60

PRON No. 1A2250041A1A

DISCLAIMER

The findings in this report are not to be construed as an official Department of the Army position unless so designated by other authorized documents.

The use of trade name(s) and/or manufacture(s) does not constitute an official indorsement or approval.

DISPOSITION

Destroy this report when it is no longer needed. Do not return it to the originator.

SECURITY CLASSIFICATION OF THIS PAGE (When Data Entered)

REPORT DOCUMENTATION PAGE		READ INSTRUCTIONS BEFORE COMPLETING FORM
1. REPORT NUMBER ARLCB-TR-82020	2. GOVT ACCESSION NO.	3. RECIPIENT'S CATALOG NUMBER
4. TITLE (and Subtitle) FRACTURE MECHANICS ANALYSIS OF THE EFFECTS OF RESIDUAL STRESS ON FATIGUE LIFE		5. TYPE OF REPORT & PERIOD COVERED Final 6. PERFORMING ORG. REPORT NUMBER
7. AUTHOR(s) Joseph F. Throop		8. CONTRACT OR GRANT NUMBER(s)
9. PERFORMING ORGANIZATION NAME AND ADDRESS US Army Armament Research & Development Command Benet Weapons Laboratory, DRDAR-LCB-TL Watervliet, NY 12189		10. PROGRAM ELEMENT, PROJECT, TASK AREA & WORK UNIT NUMBERS AMCMS No. 611102H600011 DA Project No. 1L161102AH60 PRON No. 1A2250041A1A
11. CONTROLLING OFFICE NAME AND ADDRESS US Army Armament Research & Development Command Large Caliber Weapon Systems Laboratory Dover, NJ 07801		12. REPORT DATE July 1982 13. NUMBER OF PAGES 16
14. MONITORING AGENCY NAME & ADDRESS(if different from Controlling Office)		15. SECURITY CLASS. (of this report) UNCLASSIFIED 15a. DECLASSIFICATION/DOWNGRADING SCHEDULE

16. DISTRIBUTION STATEMENT (of this Report)

Approved for public release; distribution unlimited.

17. DISTRIBUTION STATEMENT (of the abstract entered in Block 20, if different from Report)

18. SUPPLEMENTARY NOTES

To be published in the ASTM Journal of Testing and Evaluation.

19. KEY WORDS (Continue on reverse side if necessary and identify by block number)

Residual Stresses
Metal Fatigue
Crack Propagation
Stress Intensity Factor Range
S-N Curve

20. ABSTRACT (Continue on reverse side if necessary and identify by block number)

It is re-emphasized here that the effect of residual stress in fatigue is analogous to but not the same as the mean stress effect from applied loads.

The inclusion of a residual stress term in the stress intensity factor range of the fatigue crack propagation rate equation permits one to use the residual stress in calculations of fatigue life estimates. Using crack shape factors

(CONT'D ON REVERSE)

20. ABSTRACT (CONT'D)

calculated for given aspect ratios of surface flaws and integrating da/dN, one obtains an equation for the S-N curve which includes the residual stress effect on fatigue performance.

This process of calculation reveals that compressive residual stress has a much stronger influence on fatigue life than tensile residual stress does, mainly because the former decreases the stress intensity factor range and increases the critical crack size while the latter only decreases the critical crack size. Numerical solution of an example illustrates an application of these concepts.

TABLE OF CONTENTS

TABLES

LIST OF ILLUSTRATIONS

INTRODUCTION

Earlier work by J. Morrow and E. S. Rowland[1-3] aptly described the effect of residual stress in fatigue as analogous to the effect of mean stress and showed that the effect of tensile mean stress is to reduce fatigue life while that of compressive mean stress is to increase fatigue life. It has subsequently been incorrectly implied by others that the effect of residual stress is the same as that of an applied mean stress. The following relationships show that they are analogous but not the same. Considering the mean and alternating components of an applied cyclic stress gives:

$$\begin{aligned} \sigma_{max} &= \sigma_{mean} + \sigma_{alt} \\ \sigma_{min} &= \sigma_{mean} - \sigma_{alt} \end{aligned} \tag{1}$$

However, combining a residual stress with an applied cyclic stress differs because the residual stress is not a function of the active loading. Thus

$$\begin{aligned} \sigma_{max} &= \sigma_{residual} + (\sigma_{mean} + \sigma_{alt}) \\ \sigma_{min} &= \sigma_{residual} + (\sigma_{mean} - \sigma_{alt}) \end{aligned} \tag{2}$$

Hence for an active loading from zero to maximum, as in a pressure vessel, where σ_{mean} is equal to the active σ_{alt}:

$$\begin{aligned} \sigma_{max} &= \sigma_{residual} + 2\,\sigma_{alt} \\ \sigma_{min} &= \sigma_{residual} \end{aligned} \tag{3}$$

---

[1]Morrow, JoDean and Sinclair, G. M., "An Analysis of Cyclic Stress Behavior for Conditions of Controlled Strain," Theoretical and Applied Mechanics Report No. 543, University of Illinois Eng. Bulletin, August 1957.

[2]Morrow, JoDean and Millan, J. F., "Influence of Residual Stress on the Fatigue of Steel," Society of Auto. Eng. TR-198 (July 1961), SAE J783, Div. 4 of the SAE Iron and Steel Technical Committee.

[3]Rowland, E. S., "Effect of Residual Stress on Fatigue," Proceedings of Tenth Sagamore Conference, Syracuse University Press, 1964, pp. 229-244.

The residual stress is continually present, whether or not the service load is acting. It must be kept in mind that a residual stress state may be biaxial at the surface of a body and may be triaxial in the interior. The principal axes of this state may or may not coincide with the axes of the principal applied stresses. These stationary aspects of residual stresses make it necessary to exercise care when including them in analytical expressions for fatigue crack growth. This report is intended to illustrate a way that the residual stress effect may be examined separately from mean-stress or R-ratio effects in fracture mechanics analysis.

FRACTURE MECHANICS ANALYSIS

Using the Paris-Erdogan[4] fatigue crack propagation rate equation

$$da/dN = \frac{1}{M} (\Delta K)^m \tag{4}$$

one can include the effect of residual stress in the fatigue life estimate for a component as illustrated in the following analysis.

The crack tip stress intensity factor K resulting from an applied loading which varies from zero to the stress level σ is given by

$$K = \gamma\sigma\sqrt{\pi a} \tag{5}$$

In a tension member $\sigma = P/A$; in a plate or beam having a section modulus Z, σ is the applied extreme fiber stress Pe/Z, where Pe is the bending moment; and in an internally pressurized cylinder of diameter ratio w = OD/ID, $\sigma = \left(\frac{2w^2}{w^2-1}\right)p$

[4]Paris, P. C., "The Fracture Mechanics Approach to Fatigue," Fatigue, An Interdisciplinary Approach, Burke, J. J., Reed, N. L., Weiss, V., Editors, Proceedings Tenth Sagamore Army Materials Research Conference, Syracuse University Press (1964), pp. 107-132.

from the hoop stress and the pressure in the crack, as shown by Underwood.[5] When the values for σ and γ are taken to be independent of crack depth "a" these expressions apply only for shallow crack depths.

CRACK SHAPE

For semi-elliptical surface cracks we define a shape factor as

$$SF = \frac{\gamma}{1.12} \tag{6}$$

where for a shallow straight fronted crack in a plate under tension the value of γ is 1.12, and the value of SF is unity. The values for γ for curved fronted semi-elliptical surface cracks may be calculated from expressions developed by Newman and Raju[6] for surface cracks in a plate under tension or bending loads. The values for SF for a given aspect ratio and crack depth are given in Table I.

As the crack depth increases the shape factor for any given crack shape increases under tension loading while under bending the shape factor decreases. Since most of the fatigue life of a component is expended at shallow crack depth we may use the values of SF for $a \ll B$ as constants independent of crack depth for a good first approximation in either tension or bending in the following analysis. Considering SF as independent of the crack depth permits a relatively simple integration of da/dN. More precise life estimates may be made by taking into account the variation of SF as crack depth increases.

---

[5] Underwood, J. H., "Stress Intensity Factors For Internally Pressurized Thick-Wall Cylinders," Stress Analysis and Growth of Cracks, Proceedings of 1971 National Symposium on Fracture Mechanics, Part I, ASTM STP 513, American Society for Testing and Materials, (1972), pp. 59-70.

[6] Newman, J. C. and Raju, I. S., "Analysis of Surface Cracks in Finite Plates Under Tension or Bending Loads," NASA-TP-1578, (1979).

TABLE I. SHAPE FACTOR (SF) FROM NEWMAN AND RAJU EQUATIONS[6]

Crack Front Shape	Aspect Ratio a/2c	Tension or Bending SF @ $a \ll B$	@ $a = 0.2W$ Tension SF	Bending SF
Straight	0	1.000	1.000	1.000
Very long curve	.005	0.999	1.144	0.888
Long curve	.10	0.937	0.993	0.757
Semi-elliptical	.33	0.719	0.732	0.543
Semicircular	.50	0.586	0.591	0.432

NOTE: For very small crack depth, ($a \ll B$), the value of SF is given by

$$SF = \frac{1}{1.13} \left[\frac{1.13 - 0.09(a/c)}{\sqrt{1 + 1.464(a/c)^{1.65}}} \right]$$

for either tension or bending.

INCLUDING RESIDUAL STRESS

For residual stress which decreases linearly with depth from the value σ_o at the surface of the part to a zero value at the depth a_o as shown in Figure 1, the crack tip stress intensity factor is given by Underwood and Throop[7] as

$$K = (1.12 - 0.68 \frac{a}{a_o}) \sigma_o \sqrt{\pi a} \qquad (7)$$

[6]Newman, J. C. and Raju, I. S., "Analysis of Surface Cracks in Finite Plates Under Tension or Bending Loads," NASA-TP-1578, (1979).

[7]Underwood, J. H. and Throop, J. F., "Surface Crack K-Estimates and Fatigue Life Calculations in Cannon Tubes," Part-Through Crack Fatigue Life Predictions, ASTM STP 687, J. B. Chang, Ed., American Society for Testing and Materials, (1979), pp. 195-210.

for a straight fronted crack. Applying a shape factor for a semi-elliptical surface crack subjected to the superposition of applied stress $\Delta\sigma$ and residual stress σ_o gives

$$K_{max} = SF \left\{1.12\left(1 + \frac{\sigma_o}{\Delta\sigma}\right) - \frac{0.68\sigma_o \; a}{(\Delta\sigma) \; a_o}\right\}\Delta\sigma\sqrt{\pi a} \qquad (8)$$

which is of the form

$$K_{max} = SF \left\{A + Ba\right\}\Delta\sigma\sqrt{\pi a} \qquad (9)$$

If there is no residual stress, $\sigma_o = 0$, $A = 1.12$ and $B = 0$. When the residual stress is compression, σ_o is negative, hence A is smaller than 1.12 and B is positive, with the result that K_{max} is smaller than when there is no residual stress. Conversely, when the residual stress is tension σ_o is positive, hence A is larger than 1.12 and B is negative, with the result that K_{max} is larger than when there is no residual stress.

CRITICAL CRACK DEPTH

The critical crack depth, a_c, for a given applied stress range $\Delta\sigma$ can be solved from the expression for K_{max}:

$$a_c \left\{A + Ba_c\right\}^2 = \frac{1}{\pi} \left[\frac{K_{Ic}}{(SF)\Delta\sigma} \right]^2 \qquad (10)$$

Compression residual stress increases a_c, and tension residual stress decreases a_c relative to that for $\sigma_o = 0$. The residual stress effect is expressed in the squared term $(A + Ba_c)$. The solution of equation (10) for a_c gives three roots of a cubic equation, of which the smaller is the limiting crack depth. In this expression $\Delta\sigma$ is the excursion of stress from zero to its maximum value in the load cycle.

STRESS INTENSITY FACTOR RANGE

In calculating the crack propagation rate when σ_o is compression the stress intensity factor range is

$$\Delta K = (K_{max}-0) = SF\left\{1.12\left(1 + \frac{\sigma_o}{\Delta\sigma}\right) - \frac{0.68\sigma_o\ a}{(\Delta\sigma)\ a_o}\right\}\Delta\sigma\sqrt{\pi a} \tag{11}$$

or

$$\Delta K = SF\{A + Ba\}\Delta\sigma\sqrt{\pi a} \tag{12}$$

Here ΔK is the same as K_{max} in equations (8) and (9). Since σ_o is negative the compressive residual stress reduces ΔK, and reduces the fatigue crack propagation rate and thereby extends the fatigue life beyond that for zero residual stress. If $\Delta\sigma$ is not great enough to overcome the compressive residual stress, the resulting ΔK will be negative, the crack will remain closed at maximum load, and no fatigue crack growth should take place.

When the residual stress σ_o is tension, i.e., positive, the stress intensity factor range is

$$\Delta K = K_{max} - K_{min} \tag{13}$$

where K_{max} is given by equation (8) and K_{min} is given by equation (7) multiplied by the shape factor SF. The result is that for tensile residual stress

$$\Delta K = 1.12(SF)\Delta\sigma\sqrt{\pi\alpha} \tag{14}$$

which is the same as for zero residual stress.

Thus, under tensile residual stress ΔK depends only on the range of applied stress and the crack depth, and is independent of the tensile residual stress. Therefore the fatigue crack propagation rate is relatively unaffected by tensile residual stress. Experiments by Underwood[8] have shown that tensile residual stresses produced by applying compressive overloads do not greatly affect the measurable crack growth; their affects are apparently on the initiation and early growth of the crack. However, since the critical crack depth is reduced by the tensile residual stress the fatigue life is reduced, but the effect is not as great as the increase in life that would be caused by an equal value of compressive residual stress. Moreover, tensile residual stress adds to the applied mean stress and there is a recognized effect of mean stress on fatigue crack propagation rate which is not treated here in this analysis.

S-N EQUATION

Combining equation (4) and equation (12) and assuming m = 3 gives

$$da/dN = \frac{1}{M} \left(SF\{A + Ba\}\Delta\sigma\sqrt{\pi a}\right)^3 \qquad (15)$$

or

$$\int_{N_i}^{N_f} dN = \frac{M}{(SF\sqrt{\pi})^3} \frac{1}{(\Delta\sigma)^3} \int_{a_i}^{a_f} \frac{da}{\{A + Ba\}^3 a^{3/2}} \qquad (16)$$

Integrating as suggested by Berge and Myhre[9] this is written as

$$N = (N_f - N_i) = \frac{C\ I}{(\Delta\sigma)^3} \qquad (17)$$

---

[8]Underwood, J. H. and Kapp, J. A., "Benefits of Overload for Fatigue Cracking at a Notch," <u>Fracture Mechanics Thirteenth Conference</u>, <u>ASTM STP 743</u>, Richard Roberts, Ed., <u>American Society for Testing and Materials</u>, 1981, pp. 48-62.

[9]Berge, S. and Myhre, H., "Fatigue Strength of Misaligned Cruciform and Butt Joints," <u>IIW Doc. XIII 683-77</u> and <u>Norwegian Maritime Research No. I-1977</u>, Norwegian Inst. of Technology, University of Trondheim, Norway.

where

$$I = \int_{a_i}^{a_f} \frac{da}{\{A + Ba\}^3 a^{3/2}} \tag{18}$$

and

$$C = \frac{M}{(SF\sqrt{\pi})^3} \tag{19}$$

which may be expressed in log-log form as

$$\text{Log } \Delta\sigma = - \frac{1}{3} \text{ Log } N + \frac{1}{3} (\text{Log } C + \text{Log } I) \tag{20}$$

Here the factor $-\frac{1}{3}$ is the initial slope of the log-log plot and the expression $+\frac{1}{3}$ (Log C + Log I) is the intercept at N = 1 on the graph of σ versus N. (Note: if SF is not independent of a, the term SF^3 must be included inside the integral. This may be necessary for a correct solution for deep cracks.)

When there is no residual stress, $\sigma_o = 0$, and A = 1.12 and B = 0 in equation (18) for I. Therefore the S-N graph has a uniform slope of $-\frac{1}{3}$ and an intercept of

$$\frac{1}{3} \left(\text{Log } \frac{M}{(SF\sqrt{\pi})^3} + \text{Log } \frac{2}{(1.12)^3} \left[\frac{1}{\sqrt{a_i}} - \frac{1}{\sqrt{a_f}} \right]\right) \tag{20}$$

When the residual stress is compression the value of A is smaller and the value of B is larger, and the limiting crack depth a_c is larger. The resulting value of I is increased and the intercept is raised. The initial slope remains the same, $-\frac{1}{3}$, but for decreasing $\Delta\sigma$ the slope may change because the increase of critical crack depth a_c may increase the value of a_f. Both effects result in longer life at any $\Delta\sigma$ when compressive residual stress σ_o is present.

When the residual stress is tension the integration of equation (4) combined with equation (14) results in the same slope, $-\frac{1}{3}$, as for zero residual stress but, because the failure crack depth, a_c, at any $\Delta\sigma$ is reduced by the tensile residual stress, the value of I is smaller. Therefore the intercept of the S-N graph is lowered. The net effect of tensile residual stress is a shorter fatigue life for any $\Delta\sigma$ than when no residual stress is present, but the effect is predicted to be less than for equal compressive residual stress.

These effects are illustrated on the following schematic log-log S-N graph and in the following numerical example. This example and the graph were calculated, using the equations given here, expressly to compare the relative effects of compression and tension residual stresses on the S-N curve. Therefore the life estimates do not include many other aspects that should be considered in a complete fatigue life calculation.

NUMERICAL EXAMPLE

Calculate $N = (N_f - N_i)$ for $\Delta\sigma = 100$ Ksi and for $\Delta\sigma = 65$ Ksi in bending, given $a_i = 0.002$ inch; $a/2c = 0.10$; SF = 0.937; and $K_{Ic} = 80$ Ksi$\sqrt{\text{in}}$; with $m = 3$ and $\frac{1}{M} = 3.4 \times 10^{-10}$ for martensitic AISI 4340 steel with stress in Ksi and crack depth in inches. Compare results for zero residual stress, $\sigma_o = 0$, and for residual stress with $a_o = 0.45$ inch and tensile $\sigma_o = +40$ Ksi and compression $\sigma_o = -40$ Ksi. The results are given in Table II, and the corresponding S-N curves are shown on the graph in Figure 2.

TABLE II. CALCULATED CRITICAL CRACK DEPTHS AND FATIGUE LIVES

Stress Range Ksi	Zero Residual $\sigma_o = 0$	Tensile Residual $\sigma_o = +40$	Compressive Residual $\sigma_o = -40$
$\Delta\sigma = 100$	$a_c = 0.185$ in.	$a_c = 0.105$ in.	$a_c = 0.318$ in.
	$N_f = 4.34 \times 10^4$	$N_f = 4.19 \times 10^4$	$N_f = 1.56 \times 10^5$
$\Delta\sigma = 65$	$a_c = 0.438$ in.	$a_c = 0.211$ in.	$a_c = 1.177$ in. $> a_o$ * $a_f = 0.45$ in. $= a_o$
	$N_f = 1.65 \times 10^5$	$N_f = 1.60 \times 10^5$	$N_f = 2.03 \times 10^6$

1 inch = 25.400 mm; 1 Ksi = 6.8948 MPa.

*NOTE: Since Equations (7), (8), and (10) only apply to linear variation of residual stress, when a_c calculated from Equation (10) is greater than a_o for a compressive residual stress the value of a_f in Equations (11), (16), and (18) is set equal to a_o. It is thereby assumed that the number of cycles to grow from a_o to a_f is negligible.

S-N GRAPH

The log-log graph in Figure 2 shows that for the stress range between 65 to 100 Ksi (448 to 690 MPa) the tensile residual stress causes very little reduction of fatigue life, but the compressive residual stress causes considerable increase in fatigue life compared to the zero residual stress condition. Also the graph for compression residual stress is tending to curve toward a fatigue limit at about 55 Ksi (379 MPa) stress range. In real materials these tendencies are known to affect both the crack propagation threshold and the fatigue crack rate and fatigue life.

This analysis is approximate because it does not include effects of the applied mean stress or the changes in either shape factor or residual stress distribution as functions of the depth of crack. However, the latter two changes are nearly negligible in the very early portion of crack growth, wherein most of the fatigue life is spent, and the solution is therefore meaningful.

CONCLUSION

Much work remains to be done in developing quantitative relationships for expressing the effects of residual stresses in fatigue for purposes of obtaining accurate fatigue life estimation and for use in design procedures. Many aspects of residual stress effects in fatigue behavior have been merely mentioned in this report and many other aspects worthy of consideration have been omitted entirely.

The relaxation of residual stresses during the service life, vibratory stress relief, effects of peak overloads in service, effects of prior damage, residual stress effects on initiation of fatigue damage or cracks, contact fatigue, and heat treatment effects are subjects that have been suggested for investigation. Furthermore, the specification of methods for evaluating the effects of residual stress on fatigue performance and for controlling the magnitude of residual stresses within permissible limits need to be addressed.

REFERENCES

1. Morrow, JoDean and Sinclair, G. M., "An Analysis of Cyclic Stress Behavior for Conditions of Controlled Strain," Theoretical and Applied Mechanics Report No. 543, University of Illinois Eng. Bulletin, August 1957.
2. Morrow, JoDean and Millan, J. F., "Influence of Residual Stress on the Fatigue of Steel," Society of Auto. Eng. TR-198 (July 1961), SAE J783, Div. 4 of the SAE Iron and Steel Technical Committee.
3. Rowland, E. S., "Effect of Residual Stress on Fatigue," Proceedings of Tenth Sagamore Conference, Syracuse University Press, 1964, pp. 229-244.
4. Paris, P. C., "The Fracture Mechanics Approach to Fatigue," <u>Fatigue, An Interdisciplinary Approach</u>, Burke, J. J., Reed, N. L., Weiss, V., Editors, Proceedings Tenth Sagamore Army Materials Research Conference, Syracuse University Press (1964), pp. 107-132.
5. Underwood, J. H., "Stress Intensity Factors For Internally Pressurized Thick-Wall Cylinders," <u>Stress Analysis and Growth of Cracks</u>, Proceedings of 1971 National Symposium on Fracture Mechanics, Part I, ASTM STP 513, American Society for Testing and Materials, (1972), pp. 59-70.
6. Newman, J. C. and Raju, I. S., "Analysis of Surface Cracks in Finite Plates Under Tension or Bending Loads," NASA-TP-1578, (1979).
7. Underwood, J. H. and Throop, J. F., "Surface Crack K-Estimates and Fatigue Life Calculations in Cannon Tubes," <u>Part-Through Crack Fatigue Life Predictions</u>, <u>ASTM STP 687</u>, J. B. Chang, Ed., American Society for Testing and Materials, (1979), pp. 195-210.

8. Underwood, J. H. and Kapp, J. A., "Benefits of Overload for Fatigue Cracking at a Notch," Fracture Mechanics Thirteenth Conference, ASTM STP 743, Richard Roberts, Ed., American Society for Testing and Materials, 1981, pp. 48-62.

9. Berge, S. and Myhre, H., "Fatigue Strength of Misaligned Cruciform and Butt Joints," IIW Doc. XIII 683-77 and Norwegian Maritime Research No. 1-1977, Norwegian Inst. of Technology, University of Trondheim, Norway.

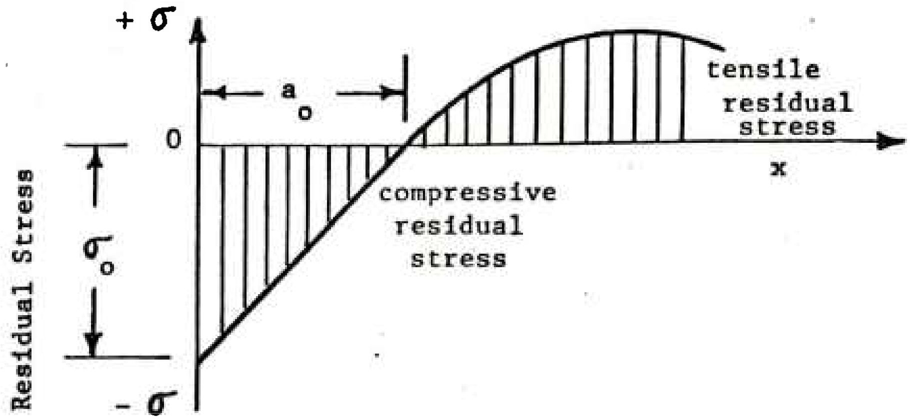

Figure 1. The idealized variation of residual stress with depth x from the surface of a component.

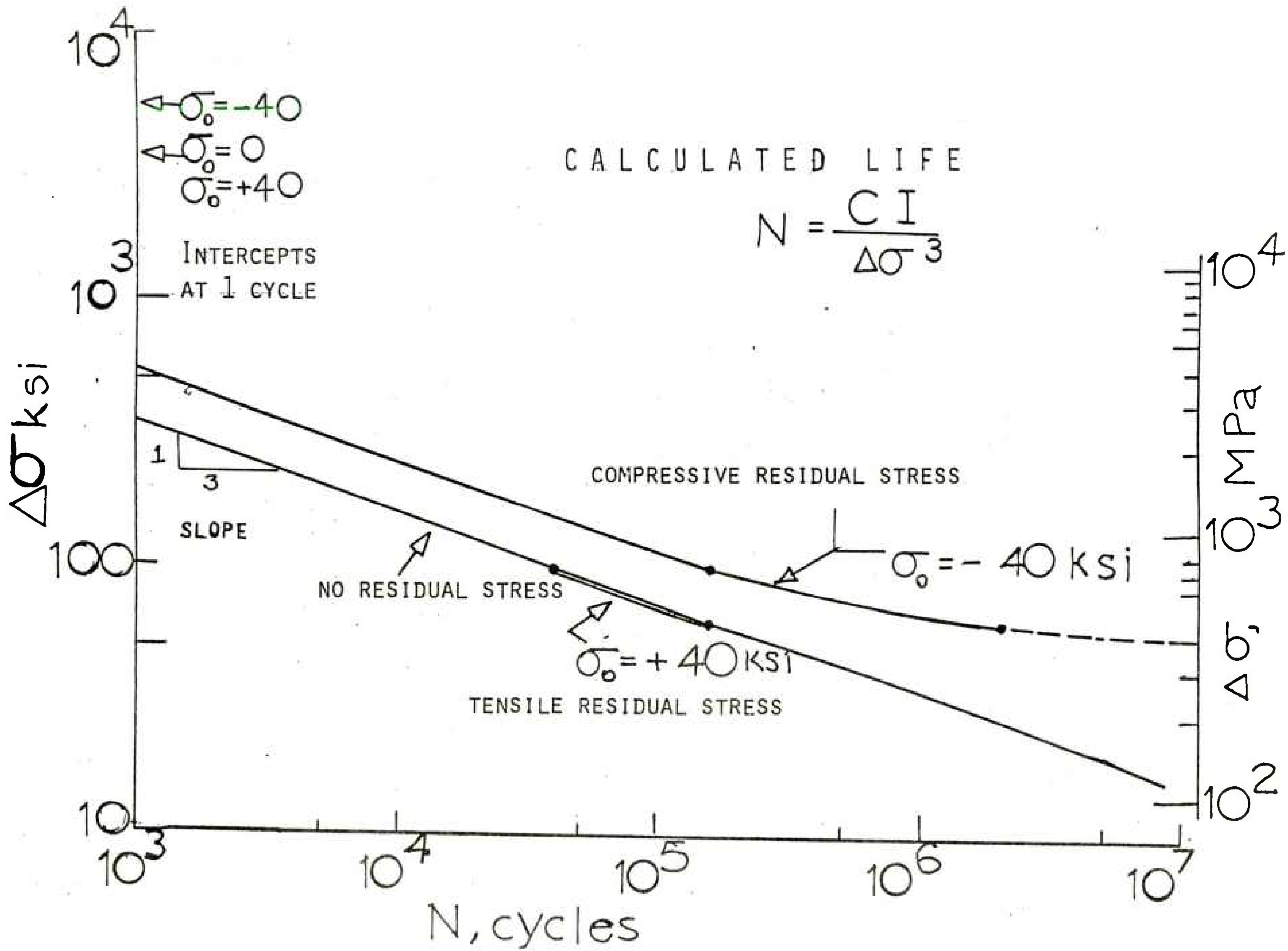

Figure 2. A fatigue S-N curve on a log-log plot of $\Delta\sigma$ versus N illustrating the calculated idealized-effects of a tensile residual stress and an equal compressive residual stress compared with zero residual stress.

TECHNICAL REPORT INTERNAL DISTRIBUTION LIST

	NO. OF COPIES
COMMANDER	1
CHIEF, DEVELOPMENT ENGINEERING BRANCH	1
ATTN: DRDAR-LCB-DA	1
-DM	1
-DP	1
-DR	1
-DS (SYSTEMS)	1
-DS (ICAS GROUP)	1
-DC	1
CHIEF, ENGINEERING SUPPORT BRANCH	1
ATTN: DRDAR-LCB-SE	1
-SA	1
CHIEF, RESEARCH BRANCH	2
ATTN: DRDAR-LCB-RA	1
-RC	1
-RM	1
-RP	1
TECHNICAL LIBRARY ATTN: DRDAR-LCB-TL	5
TECHNICAL PUBLICATIONS & EDITING UNIT ATTN: DRDAR-LCB-TL	2
DIRECTOR, OPERATIONS DIRECTORATE	1
DIRECTOR, PROCUREMENT DIRECTORATE	1
DIRECTOR, PRODUCT ASSURANCE DIRECTORATE	1

NOTE: PLEASE NOTIFY DIRECTOR, BENET WEAPONS LABORATORY, ATTN: DRDAR-LCB-TL, OF ANY REQUIRED CHANGES.

TECHNICAL REPORT EXTERNAL DISTRIBUTION LIST

	NO. OF COPIES
ASST SEC OF THE ARMY RESEARCH & DEVELOPMENT ATTN: DEP FOR SCI & TECH THE PENTAGON WASHINGTON, D.C. 20315	1
COMMANDER US ARMY MAT DEV & READ. COMD ATTN: DRCDE 5001 EISENHOWER AVE ALEXANDRIA, VA 22333	1
COMMANDER US ARMY ARRADCOM ATTN: DRDAR-LC	1
-LCA (PLASTICS TECH EVAL CEN)	1
-LCE	1
-LCM	1
-LCS	1
-LCW	1
-TSS (STINFO) DOVER, NJ 07801	2
COMMANDER US ARMY ARRCOM ATTN: DRSAR-LEP-L ROCK ISLAND ARSENAL ROCK ISLAND, IL 61299	1
DIRECTOR US ARMY BALLISTIC RESEARCH LABORATORY ATTN: DRDAR-TSB-S (STINFO) ABERDEEN PROVING GROUND, MD 21005	1
COMMANDER US ARMY ELECTRONICS COMD ATTN: TECH LIB FT MONMOUTH, NJ 07703	1
COMMANDER US ARMY MOBILITY EQUIP R&D COMD ATTN: TECH LIB FT BELVOIR, VA 22060	1
COMMANDER US ARMY TANK-AUTMV R&D COMD ATTN: TECH LIB - DRDTA-UL	1
MAT LAB - DRDTA-RK WARREN, MICHIGAN 48090	1
COMMANDER US MILITARY ACADEMY ATTN: CHMN, MECH ENGR DEPT WEST POINT, NY 10996	1
US ARMY MISSILE COMD REDSTONE SCIENTIFIC INFO CEN ATTN: DOCUMENTS SECT, BLDG 4484 REDSTONE ARSENAL, AL 35898	2
COMMANDER REDSTONE ARSENAL ATTN: DRSMI-RRS	1
-RSM ALABAMA 35809	1
COMMANDER ROCK ISLAND ARSENAL ATTN: SARRI-ENM (MAT SCI DIV) ROCK ISLAND, IL 61299	1
COMMANDER HQ, US ARMY AVN SCH ATTN: OFC OF THE LIBRARIAN FT RUCKER, ALABAMA 36362	1
COMMANDER US ARMY FGN SCIENCE & TECH CEN ATTN: DRXST-SD 220 7TH STREET, N.E. CHARLOTTESVILLE, VA 22901	1
COMMANDER US ARMY MATERIALS & MECHANICS RESEARCH CENTER ATTN: TECH LIB - DRXMR-PL WATERTOWN, MASS 02172	2

NOTE: PLEASE NOTIFY COMMANDER, ARRADCOM, ATTN: BENET WEAPONS LABORATORY, DRDAR-LCB-TL, WATERVLIET ARSENAL, WATERVLIET, N.Y. 12189, OF ANY REQUIRED CHANGES.

TECHNICAL REPORT EXTERNAL DISTRIBUTION LIST (CONT.)

	NO. OF COPIES
COMMANDER US ARMY RESEARCH OFFICE P.O. BOX 12211 RESEARCH TRIANGLE PARK, NC 27709	1
COMMANDER US ARMY HARRY DIAMOND LAB ATTN: TECH LIB 2800 POWDER MILL ROAD ADELPHIA, MD 20783	1
DIRECTOR US ARMY INDUSTRIAL BASE ENG ACT ATTN: DRXPE-MT ROCK ISLAND, IL 61299	1
CHIEF, MATERIALS BRANCH US ARMY R&S GROUP, EUR BOX 65, FPO N.Y. 09510	1
COMMANDER NAVAL SURFACE WEAPONS CEN ATTN: CHIEF, MAT SCIENCE DIV DAHLGREN, VA 22448	1
DIRECTOR US NAVAL RESEARCH LAB ATTN: DIR, MECH DIV CODE 26-27 (DOC LIB) WASHINGTON, D.C. 20375	1 1
NASA SCIENTIFIC & TECH INFO FAC P.O. BOX 8757, ATTN: ACQ BR BALTIMORE/WASHINGTON INTL AIRPORT MARYLAND 21240	1

	NO. OF COPIES
COMMANDER DEFENSE TECHNICAL INFO CENTER ATTN: DTIA-TCA CAMERON STATION ALEXANDRIA, VA 22314	12 (2-LTD)
METALS & CERAMICS INFO CEN BATTELLE COLUMBUS LAB 505 KING AVE COLUMBUS, OHIO 43201	1
MECHANICAL PROPERTIES DATA CTR BATTELLE COLUMBUS LAB 505 KING AVE COLUMBUS, OHIO 43201	1
MATERIEL SYSTEMS ANALYSIS ACTV ATTN: DRXSY-MP ABERDEEN PROVING GROUND MARYLAND 21005	1

NOTE: PLEASE NOTIFY COMMANDER, ARRADCOM, ATTN: BENET WEAPONS LABORATORY, DRDAR-LCB-TL, WATERVLIET ARSENAL, WATERVLIET, N.Y. 12189, OF ANY REQUIRED CHANGES.